The Egyptian Journal of Remote Sensing and Space Sciences (2015) 18, 235–250

HOSTED BY

ELSEVIER

National Authority for Remote Sensing and Space Sciences

The Egyptian Journal of Remote Sensing and Space Sciences

www.elsevier.com/locate/ejrs
www.sciencedirect.com

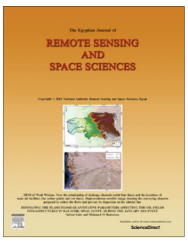

RESEARCH PAPER

GIS based Grid overlay method versus modeling approach – A comparative study for landslide hazard zonation (LHZ) in Meta Robi District of West Showa Zone in Ethiopia

Tarun Kumar Raghuvanshi [a,*], **Lensa Negassa** [a,1], **P.M. Kala** [b,2]

[a] *School of Earth Sciences, College of Natural Sciences, Addis Ababa University, PO Box 1176, Addis Ababa, Ethiopia*
[b] *Department of Geography, K.G.K. P.G. College, Moradabad, U.P., India*

Received 9 December 2014; revised 7 June 2015; accepted 31 August 2015
Available online 26 September 2015

KEYWORDS

Grid overlay;
GIS modeling;
Landslide Susceptibility Index;
Landslide hazard evaluation

Abstract The present study area is located in Meta Robi District of West Showa Zone in Oromiya Regional State in Ethiopia. The main objective of the present study was to evaluate landslide hazard zonation (LHZ) by utilizing 'Grid overlay' and 'GIS modeling' approaches. Also, it was attempted to know the effectiveness of the two methods. The methodology followed was based on the analysis of past landslides in the area. For the present study six causative factors namely; slope material, slope, aspect, elevation, land use and land cover and groundwater surface traces were considered. Later, Landslide Susceptibility Index (LSI) was computed based on the relative influence of causative factors on past landslides. For the 'Grid overlay' method a grid with cells 10 m by 10 m was overlaid over the study area and later it was geo-processed to delineate various sub-classes of each causative factor. LSI values were assigned to each sub-causative factor within each grid cell and a 'Total Landslide Susceptibility Index' was calculated to produce the LHZ map. For 'GIS modeling' the same causative factors and similar LSI values were utilized. In the case of LHZ map prepared by the 'Grid overlay' method about 82% of past landslides fall within 'very high hazard' or 'high hazard' zones whereas in the case of 'GIS modeling' about 95% of past landslides fall within 'very high hazard' or 'high hazard' zones. Finally, the validation showed that 'GIS modeling' produced better LHZ map. Also, 'Grid overlay' method is more tedious and time consuming as compared to GIS modeling.

* Corresponding author. Tel.: +251 911 875983.
E-mail addresses: tkraghuvanshi@gmail.com, tarunraghuvanshi@yahoo.com (T.K. Raghuvanshi), lensanegassa@yahoo.com (L. Negassa), drpmkala@gmail.com (P.M. Kala).
[1] Tel.: +251 917804038.
[2] Tel.: +91 9557141353.

Peer review under responsibility of National Authority for Remote Sensing and Space Sciences.

http://dx.doi.org/10.1016/j.ejrs.2015.08.001

1. Introduction

The most devastating natural hazard in mountainous terrain are landslides that has accounted for heavy loss and injury to human life and damaged property and infrastructure in millions of dollars throughout the world (Raghuvanshi et al., 2014; Pan et al., 2008; Kanungo et al., 2006; Crozier and Glade, 2005; Dai et al., 2002; Parise and Jibson, 2000; Varnes,1996). Landslide is a complex process which is resulted because of intrinsic parameters and the external parameters which triggers the process of landslide. The intrinsic parameters which govern the stability condition of the slope are; geological factors (lithology or soil type, structural discontinuity characteristics, shear strength of the material, groundwater condition and its effect), geometry of slope (slope inclination, aspect, elevation and curvature) and land use and land cover (Raghuvanshi et al., 2014; Wang and Niu, 2009; Ayalew et al., 2004; Anbalagan, 1992; Hoek and Bray, 1981). The major natural parameters which, trigger the instability in slopes are mainly seismicity (Bommer et al., 2002; Keefer, 2000; Parise and Jibson, 2000) rainfall (Dahal et al., 2006; Dai and Lee, 2001; Collison et al., 2000) and manmade activities (Raghuvanshi et al., 2014; Wang and Niu, 2009).

Over the past several years, for landslide hazard evaluation, prediction and zonation several researchers have proposed a number of approaches. Some of these approaches are based on field judgment and the experience of an evaluator, commonly placed under the category of expert evaluation approaches. Some of these approaches are as proposed by Raghuvanshi et al. (2014), Guzzetti et al. (1999), Turrini and Visintainer (1998), Sarkar et al. (1995), Anbalagan (1992), Pachauri and Pant (1992), etc. The second type of approach used for landslide hazard evaluation is the statistical approach. In these approaches attempts are made to evaluate spatial landslide instability based on the relationship in between the active landslide activities and the instability causative parameters (Carrara et al., 1992). In these approaches the general rules are developed statistically with the relative contribution of instability parameters on active landslide occurrence (Westen, 1994). The landslide hazard can be deduced by applying weights, deduced statically to be applied to each factor subclass (Dai and Lee, 2001). The third type of approach which provides the quantitative results for landslide hazard is the deterministic approach. This technique provide hazard in absolute values in the form of safety factors, or the probability. The deterministic methods are too detailed and can only be applied to individual slopes (Fall et al., 2006). These techniques require detailed slope geometry, geological and geotechnical data sets. Each of these approaches has its own advantages and disadvantages over others (Raghuvanshi et al., 2014; Fall et al., 2006; Kanungo et al., 2006; Casagli et al., 2004; Guzzetti et al., 1999; Leroi, 1997). Each of these methods has some degree of uncertainty owing to parameters considered or methods by which parameter data are acquired (Carrara et al., 1995).

Most of the techniques used for landslide hazard evaluation and zonation require a large volume of data on various causative factors. The type and extent of data required for causative factors may depend on the scale of the study and the technique followed for hazard evaluation. For analysis purpose a large volume of data can conveniently be acquired, stored and analyzed in digital form using the Geographical Information System (GIS) (Lan et al., 2004; Carrara et al., 1995). Several GIS-based analysis techniques for landslide hazard zonation have been proposed since the advancement of GIS technology (Peng et al., 2012; Kanungo et al., 2006; Ayalew and Yamagishi, 2004; Sarkar and Kanungo, 2004; Lee and Min, 2001; Carrara et al., 1995, etc.

The highlands of Ethiopia witness a number of landslides and related slope instability problems during every rainy season. In the past, several published or unpublished studies following analytical, qualitative or empirical approaches have been carried out in different parts of the Ethiopian Highlands (Ayele et al., 2014; Raghuvanshi et al., 2014; Ayenew and Barbieri, 2005; Ayalew and Yamagishi, 2004; Ayalew, 1999, etc. The present study area is located in highlands under Meta Robi District in the West Showa Zone in Central Ethiopia. Several landslides have occurred in the last few years in the present study area. People have been permanently displaced from their residences, as they lost their houses and farm plots. However, no published or unpublished study on landslides has been reported from the area prior to the present study. Therefore, seeing the severity of landslide related problems in the area the present research study was conducted.

The main objective of the present study was to prepare the landslide hazard zonation (LHZ) map of the study area. For LHZ map preparation 'Grid overlay' and GIS modeling approaches were followed. Later, effectiveness of the two methods in LHZ evaluation was assessed.

2. Overview of the study area

2.1. Location

The study area is located in Oromiya Regional State in West Showa Zone in the western part of the Meta Robi District in Central Ethiopia (Fig. 1). The total study area is about 74.59 sq km and is bounded by UTM co-ordinates 1049832–1039403N and 405497E–415847E. The study area is about 96 km from Addis Ababa on the way to Muger Cement Factory via Holeta Town.

2.2. Rainfall and physiography

The study area as per the National Atlas of Ethiopia falls in "*Temperate*" to "*sub-tropical*" climatic zone. In general, based on the annual rainfall distribution patterns, the study area experiences a nearly bimodal rainfall distribution. These are from February to May and from June to September. The long term rainfall data for the present study area were procured from the Inchini meteorological station which is located roughly about 20 km, south-east of the present study area and is defined by UTM co-ordinates 431825E; 1029283N. Based on the long term precipitation data, collected from the Inchini station for the years 1998–2008, the maximum mean annual precipitation was recorded for the year 2007, which was 1543 mm and the highest monthly precipitation recorded was 368.7 in July during the same year. Therefore, it may be considered that in general, the present study area receives relatively high mean annual rainfall.

The study area has highly rugged topography and can be characterized as steep terrain. The elevation ranges from

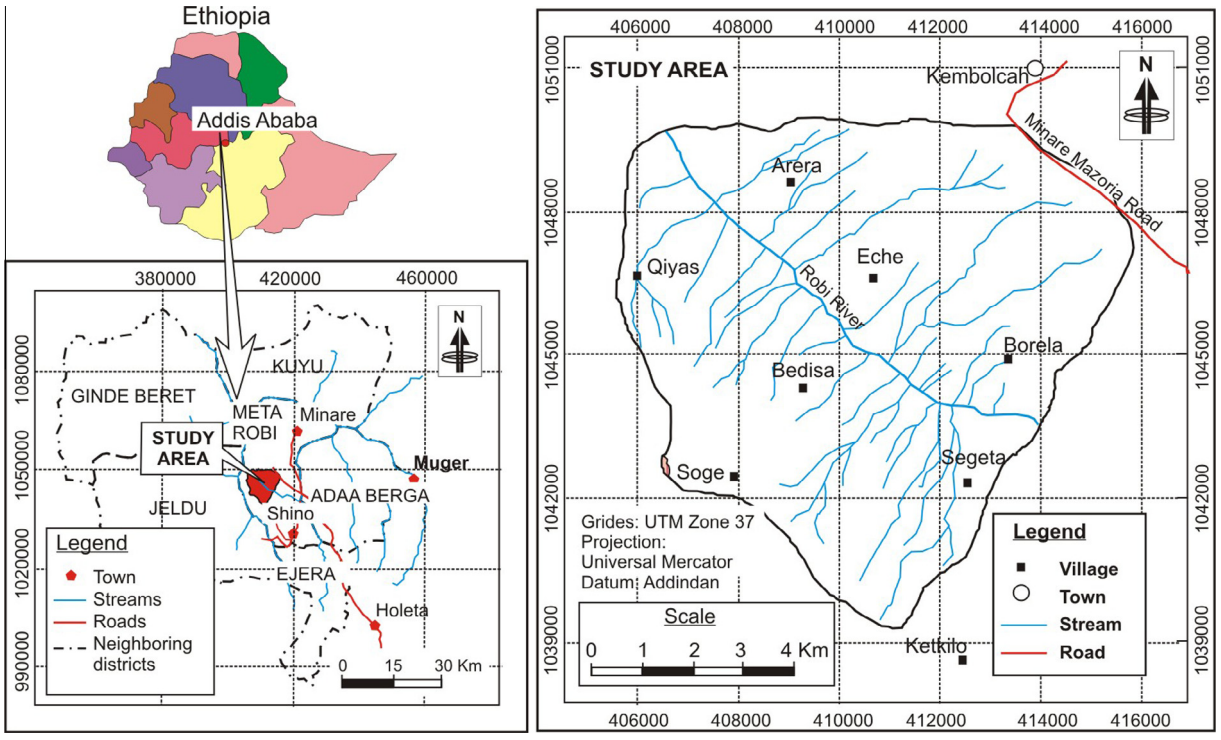

Figure 1 The study area.

1382 m to 2741 m. The Robi River is the main river in the study area which is one of the tributaries of the Muger River. In general, the area has dendritic drainage pattern.

2.3. Geology

In the present study area thick Mesozoic sedimentary rocks succession is overlaid by thick tertiary volcanic plateau basalt. The Mesozoic sedimentary rocks represent the Adigrat, Antalo and Gohatsion Formations (Fig. 2). The Adigrat Formation includes the whole succession of clastic rocks resting un-conformably on the Precambrian basement and overlain un-conformably by the Antalo Formation (Dow et al., 1971; Garland, 1980). In the study area sandstone belonging to Adigrat Formation is mainly exposed in the central portion extending toward the north-eastern parts of the study area. The Antalo Formation consists predominantly of fossiliferous yellow limestone containing thin beds of marl and calcareous shale, and occasionally arenaceous bands are also present. The majority of the study area in north-eastern and south-western portion is occupied by limestone belonging to Antalo Formation. In the study area the gypsum intercalated with thinly bedded shale belonging to Gohastion Formation is present. It overlies conformably with the lower sandstone. The rocks belonging to this formation are mainly present in the central and north-western portion of the study area. The tertiary Aiba basalts are highly fractured and jointed volcanic rocks (Assefa, 1991) which occupy mostly the north-eastern portion in the study area. The quaternary sediments in the present study area can be classified into alluvial and colluvial deposits. Quaternary alluvium is deposited mainly along stream channels, terraces and on flat plains. The alluvial sediments vary in size from sand, pebble and cobble to boulders. However, cobble to boulder size is dominant in the area.

3. Methodology

The general methodology for the present study is based on the assumption that "past is the key for future". Thus, it is believed that the conditions that have resulted in the occurrence of past landslides if prevailed again in future in other areas may possibly result in new landslides in the area (Dai and Lee, 2001). Such conditions are generally defined as; rock and soil types, slope angles and land use etc (Lan et al., 2004).

For the present study six prominent causative factors were considered for the evaluation of LHZ. These causative factors are; (i) slope material, (ii) aspect, (iii) slope, (iv) elevation, (v) land use/land cover and (vi) groundwater surface traces (Anbalagan, 1992; Ayalew et al., 2004; Raghuvanshi et al., 2014). It is further presumed that the combination of these factors might have resulted into triggering of past landslides in the present study area. The above mentioned causative factors were mainly considered based on their relative contribution in inducing instability to the slopes.

Slope material may be composed of rock mass or soils or both. In the case of rocks, rock type and its intact rock strength governs the potential for its general instability. The erodibility of rock is highly influenced by the strength of the rock (Raghuvanshi et al., 2014). Similarly, the soil type may also define its potential for its relative instability. The colluvial soils relatively possess weak shear strength as it may contain loose aggregates of fragmented rock of varied dimensions in a matrix of sandy silty clay soils. In contrast residual soils

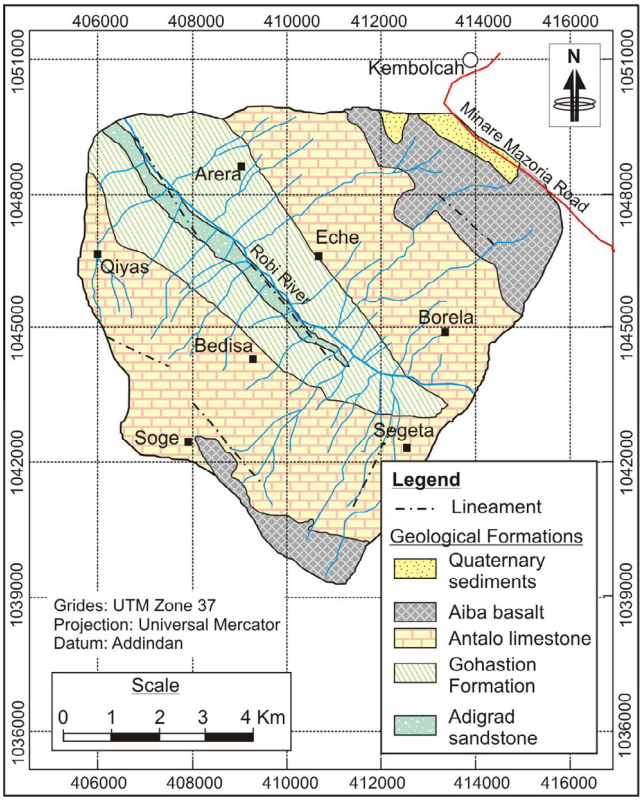

Figure 2 Geology of the study area.

are well consolidated soils and relatively possess better shear strength.

Slope gradient is important with regard to landslide initiation. The main driving force for slope instability is the gravitational pull which is directly proportional to the slope gradient. Thus, in general steeper slopes are more susceptible for instability as compared to gentler slopes.

Slope aspect strongly affects hydrologic processes via evapo-transpiration and thus affects weathering processes and vegetation and root development (Sidle and Ochiai, 2006).

The strong statistical relationships between elevation and landslide occurrence have been cited in many studies (Dai and Lee, 2002; Lineback et al., 2001; Pachauri and Pant, 1992). In general, altitude or elevation is usually associated with landslides by virtue of other factors such as slope gradient, lithology, weathering, precipitation, ground motion, soil thickness and land use.

The type of groundcover affects the stability of a slope: as the areas that are barren are more prone to erosion and weathering (Turrini and Visintainer, 1998). Barren and sparsely vegetated lands are more prone to soil erosion and slope failures (Wang and Niu, 2009).

Groundwater plays an important role in slope stability condition (Hoek and Bray, 1981). Slope stability study for hazard mapping over relatively large areas makes it difficult to have direct observations of groundwater behavior within slopes. Moreover, information on water table levels and fluctuations is rarely available. For a quick appraisal, indirect measures can be used to assess the role of groundwater (Anbalagan, 1992). For the present study groundwater surface traces (springs) and the elevation were considered to delineate the hydro-geological homogeneous zones.

Pre-field work includes data collection on topographical maps, satellite images, meteorological data and DEM data. Besides, a thorough literature review was made to know in detail about landslides types, factors responsible for landslides and various approaches available for landslide hazard evaluation. Thus, a complete conceptual framework was developed and a feasible methodology for the present study were worked out.

Field investigation and data collection were mainly undertaken to have all pertinent information about the past landslide activities and to verify various factor maps prepared during pre-field works. For past landslide activities a thorough inventory was made, where data pertaining to locations (GPS readings along the periphery of each past landslide was recorded) of landslide, possible failure mechanism by which the landslide has occurred, type of slope material involved, general slope morphology, presence of ground water traces, possible triggering factors responsible for failure and field manifestations before failure, were collected. The data and information on all these aspects were collected through hand held GPS, visual observations and through personal interviews with the local respondents.

The data and information collected from the field work were first processed and later it was used for the systematic GIS analysis. For this inventory map was prepared from the GPS location point data which were converted to polygon data by digitizing from Google-Earth image. Besides, various factor maps were reclassified to be used for later analysis. All factor maps and inventory map were brought to GIS environment so that further processing can be done. In order to evaluate the relative contribution of a sub-class of each causative factor on past landslides, Landslide Susceptibility Index (LSI) was calculated (Sarkar et al., 1995). Later, landslide hazard zonation evaluation was made.

In the present study two approaches were followed for landslide susceptibility evaluation. The first approach followed was the Grid overlay method (Carrara et al., 1995) and second approach was the GIS modeling which utilizes Model builder tool in ArcGIS. For overlay analysis a polygon grid (10×10 m) was overlaid over each prepared causative factor map and geo processing was done to know the presence or absence of each causative factor sub-class within each polygon grid cell.

Later, LSI ratings were assigned to each causative factor sub-class, falling within each polygon grid cell. Finally, within each grid cell all LSIs were summed up to get a 'Total Landslide susceptibility Index' (TLSI) which was further utilized to provide the LHZ class. In GIS modeling, LSI ratings deduced from past landslide activities and relative contribution of each causative factor were assigned and by using the weighted sum tool the final LHZ map was produced.

The LHZ maps produced by two methods were validated with past landslides recorded in the area. Further, an attempt was also made to correlate the LHZ maps produced by the 'Grid overlay' method and the 'GIS modeling' approach. Thus, a comparative analysis has been made to assess the suitability of the two approaches.

4. Landslide inventory

The Landslide hazard estimation must begin with a clear understanding on what has happened in the past in the area. This is to know what type of landslides have occurred and with what mechanism these were triggered. There needs to be a clear understanding on the possible causative and triggering factors that might have possibly resulted into landslides. The condition that has led to the past landslides in an area provides useful information for possible locations for future landslides (Lan et al., 2004; Dai et al., 2002).

During the field investigation a thorough inventory was made for the past landslide activities. As a part of this, inventory data pertaining to the location, dimension, type of failure, material involved in the landslides were collected. The field investigations pertaining to landslide inventory data collection were post landslide activities. All existing landslides in the study area were identified through traverse mapping and necessary observations were made during the field investigations. As such no systematic historical records on these landslides are maintained by the local administration. However, through predefined questionnaires local respondents were interviewed for the landslide occurrence period, possible triggering factors and any instability manifestations prior to such events; such as tension cracks, distress in slope mass etc.

In the present study area 23 past landslides were recognized. These were classified into four types of prominent failure modes; fall, translational, rotational and complex mode of failures. Rotational slides were observed at 14 locations and mostly these failure modes were observed in colluvial and alluvial soils, which formed mostly gentle slopes, though at few places they were present in relatively flat slopes. Transitional mode of failure was observed at 5 locations and at all such locations the material involved in failure was colluvial. At 3 locations the slopes failed with complex mode and material involved was highly disintegrated weathered limestone and alluvium. Only at one location 'fall' mode of failure was observed in steep slope formed by limestone.

5. Data preparation and computation

The inventory data on past landslides in the form of GPS locations, observed along the periphery of landslides were processed. Later, with the help of Google image polygon data were created for past landslides. Later, this vector map was converted to raster by using vector to raster conversion tool in ArcGIS for further computations. The landslide inventory map is presented in Fig. 3.

The stability of a slope is mainly governed by the causative intrinsic parameters (Raghuvanshi et al., 2014; Wang and Niu, 2009; Ayalew et al., 2004; Anbalagan, 1992). The causative factors considered for the present study are; slope material, slope, aspect, elevation, land use and land cover and groundwater surface traces. The various sources used to prepare spatial data sets for these causative factors are presented in Table 1.

The lithological rock map of the present study area was prepared from the Geological map (NC-37-10) prepared by the Geological Survey of Ethiopia' (GSE) at a scale of 1:250,000. The soil map of the study area was adopted from the report of Food and Agriculture Organization of the United Nations

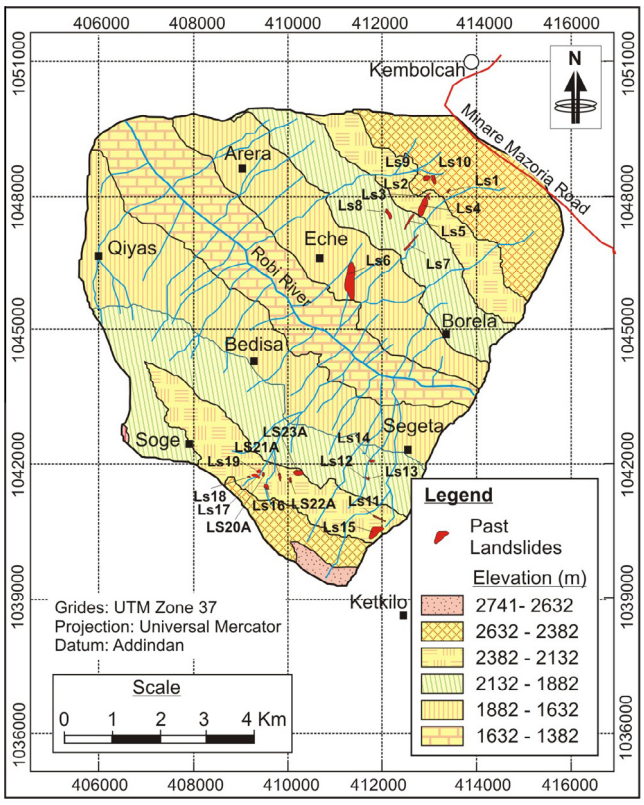

Figure 3 Landslide inventory map.

Table 1 Causative factors and their respective data sources.

Causative factors	Source
Slope material	Geological map (NC-37-10) with a scale of 1:250,000 and soil map from FAO, 1997 with suitable modifications made in field with visual observations
Slope Aspect Elevation	DEM Data of 30 m resolution ASTER elevation data set
Land use/land cover	Land sat + ETM Satellite image and field observations
Ground water surface traces	GPS location recorded for springs during Field investigation

(FAO, 1997) and was modified during the present field investigation. For the present study the lithological rock map and the soil material were mapped together and is named as 'slope material' map (Fig. 4a).

The factors; slope, aspect and elevation were deduced from digital elevation model (DEM) at a resolution of 30 m which was obtained from the ASTER elevation data set. For this purpose, a suitable operation was applied in arcMap-GIS with the help of interpolation tools using spline to obtain a smoothened output. Later, slope, aspect and elevation were reclassified into the desired classes (Table 2; Fig. 4b–d).

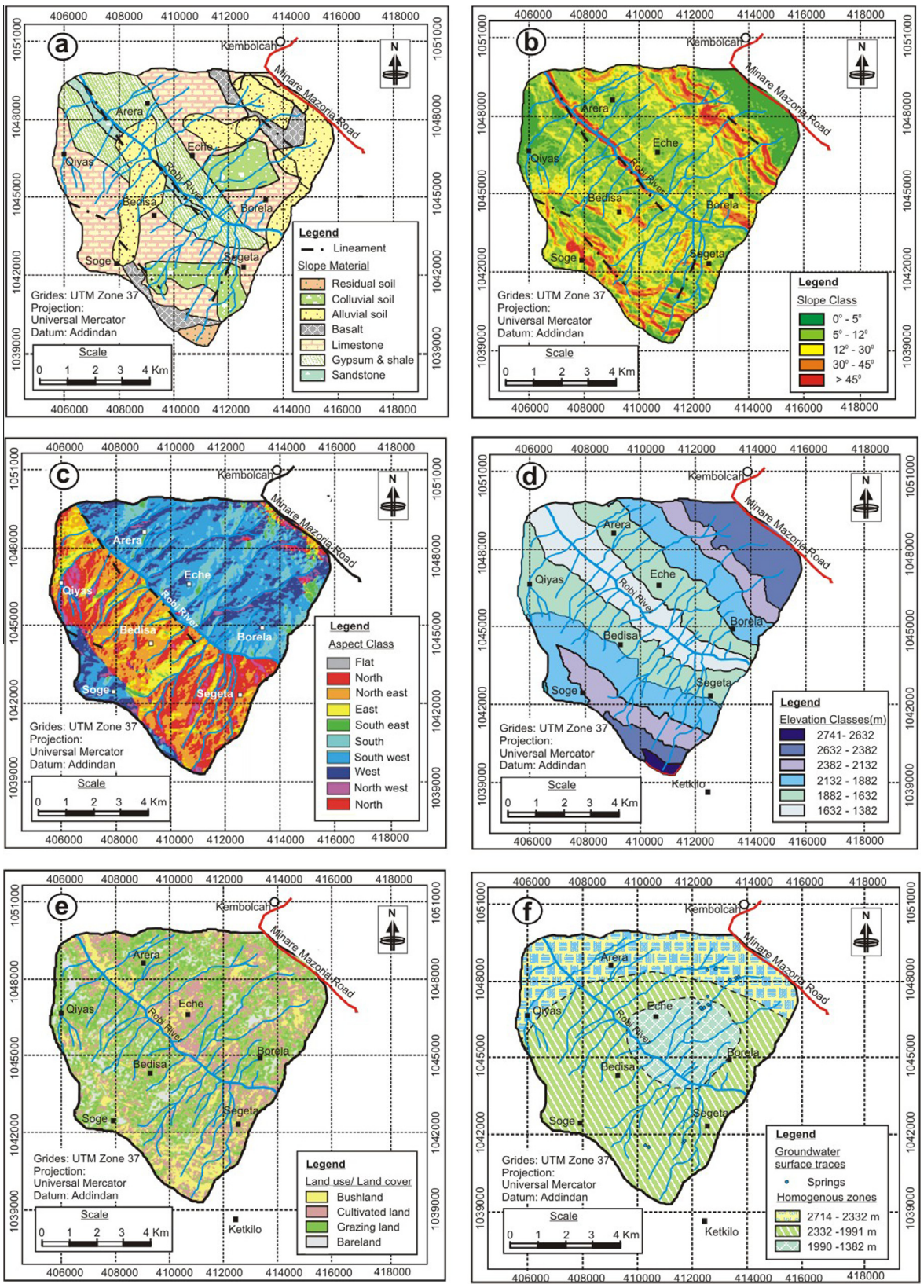

Figure 4 Causative factor maps; (a) slope material, (b) slope, (c) aspect, (d) elevation, (e) land use/land cover and (f) groundwater surface traces.

Table 2 Causative factor sub-classes and corresponding 'Landslide Susceptibility Index' (LSI).

Causative factor class	Sub-class	Pixel count of sub class in total area	Pixel count of sub-class within landslide area	Landslide % within sub class	Number of landslide occurred (%)	Landslide Susceptibility Index (LSI)
Slope material	Antalo limestone	20354	8	0.04	1.5	0.004
	Adigrat sandstone	1032	0	0.00	0	0.00
	Aiba basalt	2897	0	0.00	0	0.00
	Gohatsion Fm. (Gypsum with shale)	11236	0	0.00	0	0.00
	Quaternary sediments	310	0	0.00	0	0.00
	Residual soils	4660	0	0.00	0	0.00
	Colluvial soils	20617	456	2.20	83.3	0.22
	Alluvial soils	19374	77	0.40	15.2	0.04
Slope (deg.)	0–5	7521	4	0.05	4	0.01
	5–12	29006	144	0.50	37	0.10
	12–30	39889	127	0.30	22	0.06
	30–45	3776	18	0.50	37	0.10
	>45	288	0	0.00	0	0.00
Aspect	Flat	18	0	0.00	0	0.00
	North	8693	11	0.10	4	0.01
	Northeast	17890	45	0.30	12	0.03
	East	5073	8	0.20	8	0.02
	Southeast	1327	0	0.00	0	0.00
	South	7270	50	0.70	28	0.07
	Southwest	22759	130	0.60	24	0.06
	West	9824	15	0.20	8	0.02
	Northwest	3684	5	0.10	4	0.01
	North	3942	11	0.30	12	0.03
Elevation (m)	1382–1632	14433	0	0.00	0	0.00
	1632–1882	24906	74	0.005	35	0.001
	1882–2132	19641	16	0.0008	6	0.00016
	2132–2382	10123	76	0.0075	52	0.0015
	2382–2632	10705	12	0.001	7	0.0002
	2632–2741	672	0	0.00	0	0.00
Land use/land cover	Bush land	12337	34	0.27	22	0.081
	Cultivated land	28421	118	0.40	32	0.12
	Grazing land	30490	104	0.30	24	0.09
	Bare land	9232	25	0.27	22	0.081
Ground-water surface trace zones	1382–1990 m	6458	76	1.20	70	0.12
	1991–2332 m	25732	81	0.30	18	0.03
	2333–2714 m	11684	17	0.20	12	0.02

In the present study the interpretation and classification for land use and land cover were carried out through false color composite of Landsat ETM + for the year 2010 and a combination of bands 5, 3 and 2 of red, blue and green, respectively were used. Further, the training pixels were controlled with Google Earth image. The prepared map was verified in the field by taking Garmin GPS points. For this using ERDAS Imagine software, 26 points (GPSs) were selected from each classified group to be checked in the field. Later, some more points were selected in the field, particularly at those locations where past landslides have occurred, and were later cross checked with the image. Supervised classification was done in ERDAS Imagine and land use and land cover map of the area were prepared in Arcmap (Fig. 4e; Table 2).

Slope stability studies for hazard mapping over relatively large areas make it difficult to have direct observations of groundwater behavior within slopes. Moreover, information on water table levels and fluctuations is rarely available. For a quick appraisal, indirect measures can be used to assess the role of groundwater in inducing instability to a slope. These indirect measures are the surface indications of groundwater such as; damp, wet, dripping and flowing (Anbalagan, 1992). For the present study 'groundwater surface trace' information in the form of springs was gathered in the study area.

For the 'groundwater surface trace factor map' information gathered for springs, present in the study area, was utilized. Based on the location of springs in the study area; three hydrological homogeneous zones were recognized. These were; Zone

1 (elevation 1382–1990 m), Zone 2 (elevation 1991–2332 m) and Zone 3 (elevation 2333–2714 m) (Fig. 4f; Table 2).

For further raster computations all vector maps were converted to raster by using vector to raster conversion tool in ArcGIS. Later, total pixel count was deduced for each sub-class within past landslide area and within the total study area for all causative factor data sets (Table 2).

5.1. Landslide Susceptibility Index (LSI) computation

As already mentioned, that the general assumption made for the present study was that 'the past is the key for future'. This implies that the combination of factors which were responsible for past landslide activities may again contribute for landslide activity whenever they will have similar combination in other regions in the present study area (Dai et al., 2002). Therefore, in order to evaluate the relative contribution of a sub-class of each causative factor on past landslide, Landslide Susceptibility Index (LSI) was calculated. The LSI was devised and proposed by Sarkar et al. (1995) and can be expressed as given by Eq. (1).

$$\mathrm{LSI} = \frac{\text{Landslides \% per km}^2}{100} \times \mathrm{LSV} \quad (1)$$

where; 'LSI' is the "Landslide Susceptibility Index" and 'LSV' is the "Landslide susceptibility value" which can be assigned to each of the factors, based on the relative importance of that factor in controlling the stability condition of the slope in the given area.

According to Sarkar et al. (1995) landslide % per km^2 indicates percent of landslide activities per km^2. Thus, they have considered the number of activities which may not account for area coverage of individual landslide activities. For the present study a suitable modification was made for the LSI computation. In the present case LSI is computed by considering the landslide percentage which represents the ratio between "total pixel counts of a sub-class within a Landslide" to the "total pixel count of that sub-class in the area of study". The LSI values were calculated for each sub-class of all six causative factors. For this the Raster calculator tool of ArcGIS was used. Table 2 represents the computed LSI values for each sub-class of all causative factors.

Another parameter which is required for the computation of LSI is Landslide Susceptibility Value (LSV) which can be assigned to each of the factors, based on the relative importance of that factor in inducing instability to the slope in the given area. The distribution of LSV values to respective causative factor class is on a scale of 100 and is assigned based on the relative contribution in inducing instability to the slope. It is not possible to workout relative contribution of each causative factor in quantitative terms as each causative factor may contribute differently from slope to slope. However, based on terrain evaluation and information from past landslide activities the LSV values for causative factors may be estimated. Table 3 presents the LSV values assigned to respective causative factor class.

In the present study initially all six parameters were assigned with a LSV value of 10 each and later based on their possible contribution for instability additional values were added to give order of importance to those significant factors. Thus, it may be noted from the Table 3 that the LSV value for land use and land cover is given a maximum value of 30. It implies that land use and land cover is the most prominent causative factor as compared to other factors. This was realized as past landslides occurred in all land use and land cover classes irrespective of dominance for any particular class. The landslide inventory data show that 32% of past landslide occurred in cultivated land, 22% each in bush land and barn land and 24% in grazing land. Thus, it implies that land use and land cover have better control in inducing instability to slopes. Similarly, in the case of slope the concentration of past landslides (96%) is in three classes (5°–12° (37%), 12°–30° (22%) and 30°–45° (37%)), even in extreme gentle class (0°–5°) 4% of landslides were observed. Thus, slope was assigned with the second highest LSV value of 20. Also, in case of elevation it was realized from the past landslide data that 59% landslides occurred in classes 2632–2382 m and 2382–2132 m and 41% occurred in classes 2132–1882 m and 1882–1632 m, respectively. In this case also it may be realized that landslides are not concentrated to some specific elevation class. Almost in every elevation class landslides were recognized, except for the two extreme classes. Again it implies that elevation is a significant causative factor and thus was given a LSV value of 20.

Table 3 Landslide Susceptibility Value (LSV) assigned for the different causative factors.

S. No	Causative factors	LSV value
1	Slope material	10
2	Slope	20
3	Aspect	10
4	Elevation	20
5	Land use/land cover	30
6	Ground water surface traces	10

If compared, the other causative factors such as slope material, aspect and groundwater surface trace concentration of past landslides are realized in specific sub-classes. Say, for example in the case of slope material past landslides are concentrated within colluvial (83.3%) and alluvial soils (15.2%) only. Thus, the contribution of slope material as a causative factor may not be significant for the entire study area but it may be significant to those areas where colluvial or alluvial soils are present. Therefore, a nominal LSV value of 10 was assigned to slope material. Similarly, for the same reason nominal LSV values were assigned to aspect and groundwater surface trace. Further, it is worth mentioning that the landslide susceptibility of the area does not entirely depend on the LSV value only but it will mainly depend on the Landslide percentage which represents the ratio between "total pixel counts of a sub-class within a Landslide" to the "total pixel count of that sub-class in the area of study.

5.2. Causative factor influence on past landslides

In the following paragraphs an attempt is made to assess the relative influence of causative factors with past landslide distribution in the study area.

5.2.1. Slope material

The main rock types which are present in the study area are; Adigrat sandstone, Antalo limestone, Aiba basalts and

gypsum intercalated with thinly bedded shale of Gohatsion Formation. In the present study area Aiba basalts are exposed in the upper most parts of the area and shows typical columnar jointing. Much of the north-central and south-western part of the study area is covered by Antalo limestone. The central and north-western parts are covered by gypsum and shale intercalations. Sandstones are mainly exposed in the southern parts and in a small strip that extends from the central to north-western parts of the study area (Fig. 4a). Thus, based on the prominent rock and soil types present in the present study area slope material was classified into various classes as presented in Table 2. A perusal of Table 2 clearly shows that rocks in general have not contributed for past landslides only 1.5% of landslides were observed in limestone and were mainly complex or fall types of failures. Thus, from the past landslide inventory data it can safely be concluded that the contribution of rock types is minimum in inducing landslides, it is mainly colluvial and alluvial soils which are more susceptible for instability than the rocks, as collectively 98.5% landslides occur within these soils.

5.2.2. Slope

As the slope increases, the tendency for movement increases. Thus, the slope angle is an essential parameter for landslide analysis (Ayalew and Yamagishi, 2004). As the slope angle increases, shear stress in soil or other un-consolidated material generally increases. Gentle slopes are expected to have a low frequency of landslides because they possess lower shear stresses associated with low gradients (Ahmed, 2009).

In the present study the slope angle was divided by expert opinion based on the topography of the area into five classes as; 0–5°, 5–12°, 12–30°, 30–45° and more than 45° (Fig. 4b). A perusal of Table 2 clearly shows that the highest percentage of landslide occurred in slope class 5–12° and 30–45° which accounts for 37% each. Whereas, the slope class 12–30° accounted for 22% of past landslides. Slope class 0–5° recorded only 4% of the landslides and no landslides were recorded in the slope class greater than 45°. In general, in the present area the colluvial and alluvial soils form moderate slopes that is why much of the landslides (96%) occurred within moderate slope classes.

5.2.3. Aspect

The aspect of a slope can influence landslide initiation, because it affects moisture retention and vegetation cover, and in turn soil strength and susceptibility to landslides. The amount of rainfall on a slope may also vary depending on its aspect. Slope aspect is considered to be an important factor by many researchers. In general, slope aspect can influence the distribution and density of landslides by controlling the concentration of soil moisture (Wieczorek et al., 1997) or the orientation of tectonic fractures. A variation in the degree of weathering and basal erosion due to slope aspect was also reported by Ayalew and Yamagishi (2002) with an effect on slope failure distribution.

For the present study the Aspect has been divided based on all possible geographical directions namely; (i) Flat (−1°), (ii) North (0– 22.5°), (iii) North-east (22.5–67.5°), (iv) East (67.5–112.5°), (v) South-east (112.5–157.5°), (vi) South (157.5–202.5°), (vii) South-west (202.5–247.5°), (viii) West (247.5–292.5°), (ix) North-west (292.5–337.5°), and (x) North (337.5–360°) (Fig. 4c). The results obtained (Table 2) from the reclassified map of aspect of the study area clearly shows that 28% of the landslides occurred in slopes facing toward south, 24% in South-west, 4% in North and 12% in North-east, respectively. The remaining, landsides occurred in slopes facing East (8%), West (8%) and North-west (4%) directions, respectively. This remarkably shows the concentration of landslides in slopes facing toward South and South-west directions. The possible reason for this may be related with the ground water flow direction. As observed during the field work, a good number of springs were present in the slopes facing south or South-west directions. Thus, a clear correlation can be established between aspect, groundwater flow direction and landslides in the study area.

5.2.4. Elevation

The elevation is considered to be an important causative factor which may possibly affect the slope material by weathering process (Ahmed, 2009). For the present study the elevation was sub divided by expert opinion based on the topography of the area into 6 classes: 1382–1632 m, 1632–1882 m, 1882–2132 m, 2132–2382 m, 2382–2632 m and 2632–2741 m (Fig. 4d, Table 2).

The results obtained (Table 2) from the reclassified map shows that highest percentage of landslides (52%) occurred in the elevation class of 2132–2382 m whereas, 35% of the landslides has occurred in the elevation class of 1632–1882 m. Rest of the landslides (13%) occurred in the remaining elevation classes. One of the possible causes for the concentration of the past landslides in elevation classes 2132–2382 m and 1632–1882 m can be correlated to the agricultural practices performed by the local residents at these elevation classes. As observed during the field work that most of the cultivated lands in the area are within colluvial and alluvial soils. This is a known fact that colluvial or alluvial soils are prone to instability (Raghuvanshi et al., 2014; Anbalagan, 1992) that is why a high frequency of landslides was observed in this class. In general, cultivation over slopes increases instability by increasing moisture of the soil mass due to irrigation practice. For cultivation purpose hill slopes are made flat and cut into terraced land, this is also true in the present study area. In general, such dressing of slopes into terraced design stabilizes the slopes. However, poor irrigation or inadequate cultivation practices on such terraced land may lead to excessive recharge of groundwater which may result into instability of the slope (Raghuvanshi et al., 2014). Also, to make the land cultivable the local residents indulge in deforestation which has further increased the slope instability in the area.

5.2.5. Land use and land cover

Land use and land cover is considered to be a major factor responsible for landslides. The land which is barren and sparsely vegetated is prone to weathering, erosion and slope instability (Raghuvanshi et al., 2014; Wang and Niu, 2009; Turrini and Visintainer, 1998; Anbalagan, 1992). A thick vegetated slope generally represents a stable condition as the vegetation cover prevents excess seepage of water into the slope (Arora, 1997). Also, the root system of the plants binds the soil mass and increases the shear strength of the soil mass (Turrini and Visintainer, 1998).

For the present study land use and land cover were classified into cultivated land, bare land, bush land and grazing land (Fig. 4e, Table 2). A perusal of Table 2 indicates that about 32% of past landslides occurred within cultivated land. Though bush land, grazing land and bare land accounts for 22%, 24% and 22% of past landslides, respectively. The contribution of land use and land cover classes for past landslides were roughly equal and it cannot be said conformably which land use/land cover class will be more susceptible to landslides.

5.2.6. Groundwater surface trace

Groundwater is an important factor in inducing instability to the slopes (Raghuvanshi et al., 2014). The groundwater within the discontinuities develops water pressure which results in a decrease of shear strength along the discontinuity planes (Hoek and Bray, 1981). Also, groundwater lubricates the discontinuity surfaces thus facilitating the process of rock sliding. In soil slopes after rain-fed saturation the weight of soil mass increases and thus it adds to the instability of the soil mass. Besides, groundwater helps in pore water pressure development within the soil mass which again aggravates instability (Arora, 1997).

For the present study groundwater surface traces (springs) and the elevation were considered to delineate the hydro-geological homogeneous zones. This was done to demarcate various groundwater saturated zones within the slopes. It is apparent that in areas where the spring emerges on the surface the slope mass in close vicinity will be saturated and such a saturated mass will possess less shear strength. Thus, the slope mass will be more prone to failure provided other causative factors also contribute to instability. With this understanding the present study area was divided into three hydro-geological homogeneous zones based on the location of springs and general elevation (Fig. 4f).

A perusal of Table 2 indicates that about 70% of past landslides have occurred in hydro-geological homogeneous zone 1382–1990 m. This indicates that this zone is more prone to landslides and a high frequency of past landslides must be related to the groundwater interaction with other causative factors; mainly slope material. As can be seen in Fig. 4a (Slope material map) that within hydro-geological homogeneous zone (1382–1990 m) majority of soil material is alluvial and colluvial, which is more susceptible to instability. This fact is also evident from the high frequency of past landslides in alluvial and colluvial materials within this zone (Fig. 3).

5.3. Grid overlay analysis for landslide hazard evaluation

Overlay analysis requires that first the study area must be divided into small units defined by regular boundaries and later within each small unit the relative influence of combined factors should be studied to evolve the landslide hazard (Carrara et al., 1995). Various approaches have been forwarded for delineation of such units. For instance; Anbalagan (1992) has proposed dividing the study area into individual slope facets. Slope Facet is defined as a land unit which is characterized by more or less uniform slope geometry in terms of slope inclination and slope direction (Anbalagan, 1992). Other workers suggest dividing the area into regular square grid cells (Sarkar et al., 1995). In the present study regular square grid cells with dimensions 10×10 m were considered.

For overlay analysis the entire study area was overlaid with 10×10 m polygonal grid cells. In total 7666 grid cells covered the total study area (74.59 sq km). This grid was prepared by using the AutoCAD MAP software where first the geo-referenced study area boundary was imported as a shape file and later grid with 10×10 m cells was created. Further, this grid file was exported as a shape file to be used later for overlay analysis. For overlay analysis it was required that each grid cell must have a unique ID through which geo processing with various causative factors can be performed. Thus, the '*.dbf' file component of 'grid shape file' was edited in MS-Excel and 1 to 7666 IDs were assigned to the grid cells.

5.3.1. Geo-processing of causative factors

The objective of geo-processing was to know the type and presence of sub-classes of causative factors within each grid cell. Thus, each factor map was geo-processed with the grid. Since the number of grid cells was 7666, therefore the hardware and software failed to process the data owing to the entities more than the capacity which can be handled. Thus, to facilitate the data management and processing the grid file was further sub-divided into 7 files with 1000 cells and the eighth with 666 cells (Fig. 5). Further, each of these 8 grid files was geo-processed to find intersections with each of the six causative factor themes.

The next step for geo-processing was to merge the intersection themes obtained after intersection of grid cells and the respective causative class. This was done individually for each of the causative themes by merging two intersecting themes at a time by utilizing 'merge themes' option within geo-processing tool. Thus, finally within each grid file interaction of six factor class was obtained. Fig. 6 shows the intersection of six causative factors within the grid cell with ID 118. Thus, finally six grid files were prepared where each file contained interaction of six causative factor class within each grid cell.

Next step was to merge all these files into one so that a single grid file can be obtained which contained all grid cells from 1 to 7666 ID and have an attribute table which shows all six causative factors within each cell. Thus, all 6 grid files were merged together one by one, finally to get one single file with complete data set of 1–7666 cells and an attribute table for all six causative factors within each grid cell. Fig. 7 shows the combined single grid file (1–7666 cells) with each grid cell having specific sub-classes of six causative factor classes.

After getting cumulative intersections of causative factors within each grid cell appropriate LSIs for respective sub class were assigned from Table 2. This was done by editing sub-file '*.dbf' file of cumulative intersections causative factors shape file in MS Excel. Thus, each grid cell finally got a set of six LSIs representing sub-classes of six causative factors. Later, all six LSIs were summed up to get a cumulative value, Total Landslide Susceptibility Value (TLSI) for each grid cell. Later, these TLSI values were utilized to evolve LHZ of the study area. The range of TLSI values obtained were further classified into zones of relative instability based on the field evidences. This divided the terrain into various zones of landslide susceptibility. The total distribution of TLSI values falls within a range of 0.14–1.053. Thus, from this value range of TLSI it is reasonable to say that 0.14 TLSI value represents the least

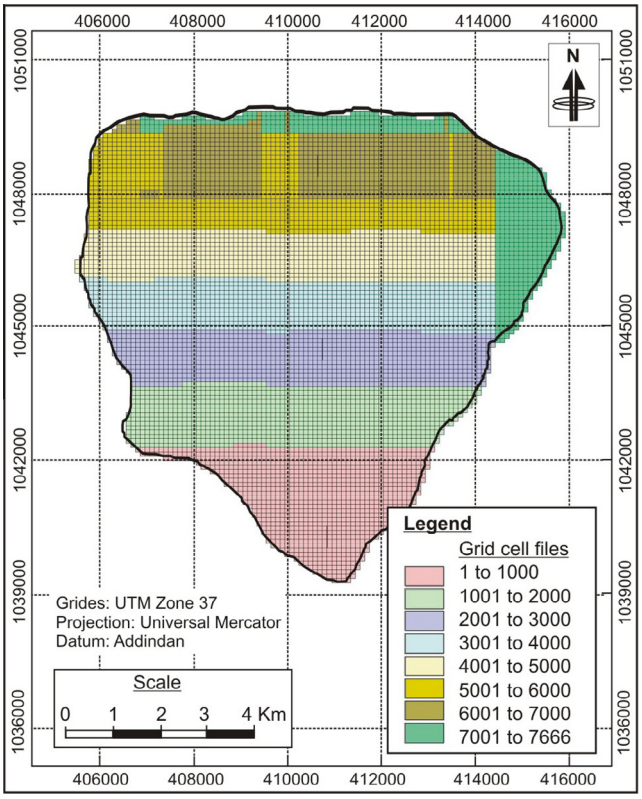

Figure 5 Grid file used for overlay analysis.

hazard and the value 1.053 indicates a very high hazard. Thus, based on the field evidence, judgment and logical consideration the landslide hazard zones were classified as; very high hazard (VHH), high hazard (HH), medium hazard (MH), low hazard (LOH) and very low hazard (VLH). By taking various distributions on trial basis a landslide hazard zonation map was prepared and for each attempt an overlay analysis was made with the past landslide data. The distribution of corresponding TLSI values for 5 hazard classes as presented in Table 4 provided the most reliable validation results and thus was considered for the final landslide hazard zonation of the study area.

5.4. Landslide hazard evaluation by GIS modeling

In the present study, in addition to grid overlay analysis for landslide hazard evaluation, an attempt has also been made to utilize the Model Builder tool of ArcGIS to develop landslide hazard zonation of the study area through modeling. The causative factors considered for LHZ map preparation by GIS Model Builder were the same as those which were utilized in grid overlay analysis. Thus, for Model builder approach the factor maps which were utilized are; slope material, slope, aspect, elevation, land use/land cover and groundwater surface trace.

In GIS modeling approach the first step was to derive all the factor maps into the model builder window. These factor maps can automatically be derived into the model builder by the software. Later, these vector maps were converted to raster by using conversion tool within Model builder. The next step followed was to reclassify six causative factor maps. Such reclassification helps to maintain the original value of sub-classes during driving the factor maps into model builder. For example; the sub-classes for the slope factors are 0–5°, 5–12°, 12–30°, 30–45° and >45°, therefore during the slope class in the model builder the values for the sub-classes are corrected by reclassification process. Thus, by using the reclassify tool in the spatial analysis tool box all the factor maps were reclassified.

Further processing required in the model builder was to assign the LSI values for the different causative factors sub-classes. For GIS modeling approach similar LSI values of sub-classes of each factor class were assigned as that was used in the 'Grid overlay' method (Table 2). After the LSI values were assigned to all causative factors sub-classes the final stage was to generate the final weighted sum raster. The process entailed combining all six raster data set. The weighted raster also stipulates that each factor raster file be assigned with a percentage weight. This is to give the relative importance of each causative factor which has to be equal to 100. In the present case the percentage weight assigned to each causative factor was considered equal to the LSV value (Table 3). Further,

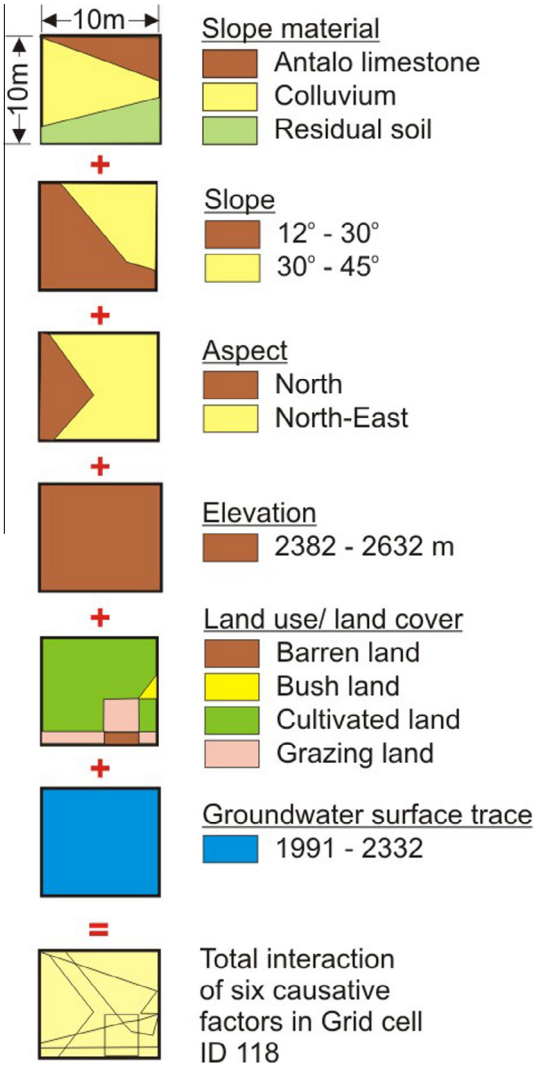

Figure 6 Intersection of six causative factors within grid cell with ID 118.

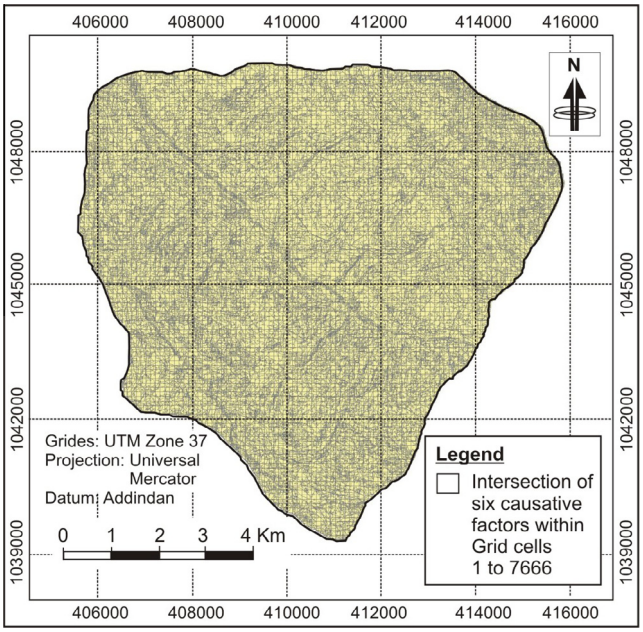

Figure 7 Geo-processed combined single grid file with each grid cell having specific sub-classes of six causative factor classes.

Table 4 Landslide hazard zones and corresponding Total Landslide Susceptibility Index (TLSI) values.

Landslide hazard zone	Zone designation	TLSI value range
Very low hazard	VLH	0.14–0.19
Low hazard	LOH	0.20–0.27
Medium hazard	MH	0.28–0.41
High hazard	HH	0.42–1.053
Very high hazard	VHH	>1.053

by using the weighted sum in the overlay tool, final weighted sum raster was generated.

Later, the final weighted sum raster was separated into five distinct hazard classes using manual breaks, based on judgement and terrain condition. In general, raster cell values ranged from a low of 260 to a high of 3400. The cell values which were separated into five distinct zones are; very low hazard (VLH), low hazard (LOH), medium hazard (MH), high hazard (HH) and very high hazard (VHH) zones with a cell value of 260–600, 600–800, 800–1200, 1200–2000 and 2000–3400, respectively. This weighted sum raster distributed for respective landslide classes was obtained on trial basis and validation of LHZ map was made with the past landslide data. The above distribution provided the most reliable validation of LHZ map and thus was finally considered to generate the LHZ map.

6. Results and discussion

Landslide inventory data in general revealed that 23 landslides had occurred in the past in the study area. All these landslides fall into four types of prominent failure modes; fall, translational and rotational slides, and complex type of failure modes.

The main triggering factor for all past landslides in the study area, as reported was rainfall as all past landslides occurred during the rainy season. As mentioned earlier the maximum mean annual precipitation in the present study area is high and the highest monthly precipitation was recorded in July. Further, all past landslides in the present study area, as reported by the respondents have taken place during the late rainy season (late August to early September) indicating a rise in groundwater level due to recharge by heavy rainfall and as a result of other favorable causative factors such as; slope material, slope gradient, land use and land cover etc. These rainfall-induced landslides in the study area possibly occurred as a result of shear strength reduction of the slope material due to saturation and development of pore water pressures within the slope mass. This fact is evident as most of the past landslides in the study area have occurred within the slopes composed of colluvial and alluvial soils.

Out of total, 83.3% of past landslides have occurred in colluvial soil slopes whereas about 15.2% landslides were observed in alluvial soils. Not many landslides were recorded from slopes formed by rocks. It is reasonable to understand that colluvial soils are loose soils which may be comprised of angular to sub-angular rock fragments of variable dimensions in a matrix of sandy silty soils. Such material possesses low shear strength and when saturated may result into washing of finer particles and may become more prone to instability (Raghuvanshi et al., 2014; Anbalagan, 1992). The high concentration of past landslides in colluvial soils in the study area is well related to the above mentioned nature of these soils.

The slope angle is an important factor in controlling the stability of slope. Steeper the slope the more the tendency for instability will be (Hoek and Bray, 1981). In the present study area steep slopes (>45°) are formed mainly by rocks, which show less frequency of landslides as compared to moderate slopes. The main reason for this is that moderate slopes in the study area are formed by colluvial and alluvial soils which are more prone for instability that is why much of the landslides (96%) occurred within moderate slope classes.

Further, it was observed that the concentration of landslides is in slopes facing toward south and south-west directions. The possible reason for this may be related with the ground water flow direction. As observed during the field work for the present study, a good number of springs were present in the slopes facing south or south-west directions, which perhaps indicates the possible groundwater flow toward south or south-west directions. Groundwater plays an important role in slope instability condition (Hoek and Bray, 1981). High frequency of landslides toward southern (28%) and south-west (24%) directions very well demonstrates the role of groundwater in inducing instability to slopes in the study area.

Most of the landslide (52%) occurred in the elevation class of 2132–2382 m whereas, 35% of the landslide has occurred in the elevation class of 1632–1882 m. One of the possible causes of high concentration of past landslides in elevation classes 2132–2382 m and 1632–1882 m can be correlated to the agricultural practices performed by the local residents at these elevation classes. Poor irrigation or inadequate cultivation practices on such terraced land may lead to excessive recharge of groundwater which may result into instability of the slope (Raghuvanshi et al., 2014).

Cultivated land showed high frequency (32%) of past landslides. Again this may be related to poor irrigation practice which might have resulted into instability of slopes. Also, cultivation land in the study area mostly comprises of colluvial or

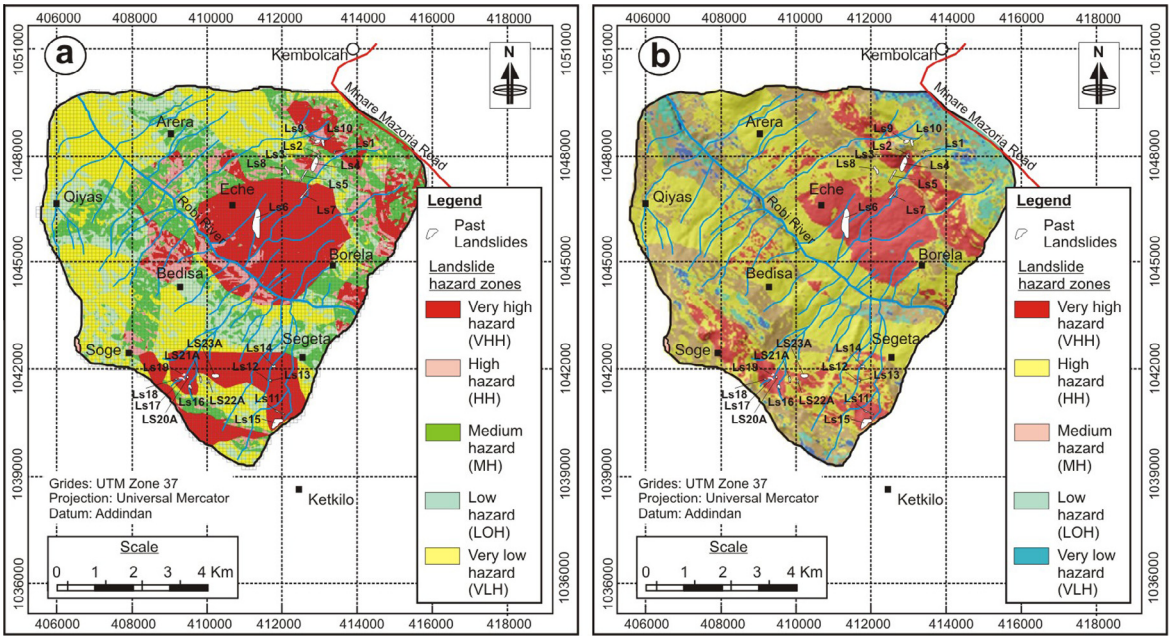

Figure 8 Landslide hazard zonation (LHZ) map (a) Grid overlay method (b) GIS modeling approach.

alluvial soils which are prone for instability (Anbalagan, 1992; Raghuvanshi et al., 2014) that is why a high frequency of landslides was observed in this class. In general, the contribution of other land use/land cover classes for past landslides in the study area is roughly equal and it cannot be said conformably that which land use/ land cover class will be more susceptible for landslides.

About 70% of past landslides has occurred in hydrogeological homogeneous zone 1382–1990 m. This indicates that this zone is more prone to landslides and a high frequency of past landslides must be related to the groundwater interaction with other causative factors. Much of this zone is occupied by colluvial and alluvial deposits which is relatively more susceptible to instability (Raghuvanshi et al., 2014).

6.1. Landslide hazard zonation by 'Grid overlay' method

The LHZ map of the study area prepared by grid overlay method (Fig. 8a) clearly shows that 19.44% of the study area has a 'very high landslide hazard' (VHH) potential and 30.78% area has 'high landslide hazard' (HH) potential. Whereas, the areas that account for 'medium hazard' (MH), 'low hazard' (LOH) and 'very low hazard' (VLH) are 41.08%, 6.48% and 2.23%, respectively.

Majority of the study area (30.64 km^2) has 'medium hazard' (MH). Medium hazard zones are mostly concentrated in the northern, western and south-western parts of the study area. Very high hazard (VHH) zone covers mostly the central, southern and south-western parts of the study area with area coverage of about 14.5 km^2. High hazard (HH) zones are relatively scattered and falls mainly in the central, north- eastern and south-western parts of the study area. The HH zones cover about 22.96 km^2 of the study area. Areas with low hazard (LOH) potential are very less (4.83 km^2) and are scattered throughout the study area. Very low hazard (VLH) areas are mostly found in northern, north-western and north-eastern parts, few scattered areas of VLH zones can also be seen in southern parts of the study area. The total area covered by VLH zone is only about 1.66 km^2 in the study area (Table 5).

6.2. Landslide hazard zonation by GIS modeling approach

LHZ map developed by modeling approach (Fig. 8b) reveals that the area is highly susceptible to landslide hazard. It shows that 21.4% of the area falls in very high hazard zone (VHH), 33.2% in high hazard (HH) zone and 34.4% in medium hazard (MH) zone. In total 54.6% of the area falls in either VHH or HH zones. Perusal of Fig. 8b and Table 5 shows that VHH zones are concentrated in the north-eastern and south-western portion of the area. The HH zones are evenly distributed in the central, north-western and south-eastern portions of the study area. The remaining medium (MH), low (LOH) and very low hazard (VLH) zones have scattered distribution in the area.

6.3. Validation of LHZ maps

The methodology followed for the present study is formulated by considering an assumption that 'past is the key for future' (Dai et al., 2002), therefore the LHZ map prepared following the said methodology must validate the past landslide activities. This implies that the past landslide activities must fall within very high hazard or high hazard zones, delineated in the prepared LHZ map. Therefore, attempts were made to overlay the past landslide inventory map over the LHZ map prepared by 'Grid overlay' method and 'GIS modeling' approach.

6.3.1. Grid overlay method

The overlay analysis of past landslides over LHZ map prepared by the 'Grid overlay' method (Table 6, Fig. 8a) revealed that out of 23 past landslide activities 14 landslides (61%) fall

Table 5 Area coverage by various landslide hazard zones in the study area.

Landslide hazard zone	Grid overlay method		GIS modeling approach	
	Area coverage in Sq. km	Percent area coverage	Area coverage in Sq. km	Percent area coverage
Very high hazard (VHH)	14.5	19.44	16.13	21.4
High hazard (HH)	22.96	30.78	24.72	33.2
Medium hazard (MH)	30.64	41.08	25.61	34.4
Low hazard (LOH)	4.83	6.48	4.81	6.5
Very low hazard (VLH)	1.66	2.23	3.32	4.5
Total area	74.59	100	74.59	100

within VHH zone whereas, 5 Landslides (21.73%) fall within HH zone. Thus, 19 landslides out of 23 fall within VHH or HH zones, which is about 82.73% of the total past landslide activities. Further, only 4 past landslides (17.39%) fall within the MH zone and none of the past landslides fall within LOH or VLH zone. That means 82.73% of past landslides show satisfactory agreement with the present LHZ map prepared by the Grid overlay method.

6.3.2. GIS modeling

Results as presented in Table 6 and Fig. 8b shows that out of 23 past landslide activities 15 landslides (65.2%) fall within VHH zone whereas, 7 Landslides (30.4%) fall within HH zone. Thus, 22 landslides out of 23 fall within VHH or HH zones, which is about 95.6% of the total past landslide activities. Further, only 1 past landslide (4.3%) fall within the MH zone and none of the past landslides fall within LOH or VLH zones. Thus, the LHZ map prepared by GIS modeling is in good agreement with the past landslides in the area.

6.4. Effectiveness of 'Grid overlay' method versus 'GIS modeling' in LHZ evaluation

The input parameters considered for the two methods were the same. In both methods six causative factors namely; slope material, slope, aspect, elevation, land use/land cover and groundwater surface traces were used. Similar sub-classes of various causative factors were used for both the methods and identical LSI values were assigned. If the results are compared, marginal variation is found in the areas depicted for various landslide hazard classes by the two methods. For both the approaches five landslide hazard classes namely; very high hazard (VHH), high hazard (HH), medium hazard (MH), low hazard (LOH) and very low hazard (VLH) were considered. The validation of LHZ maps produced by two approaches when validated with past landslide activities, shows that GIS modeling gives better validation (Table 6; Fig. 8).

Table 6 Validation of landslide hazard zonation (LHZ) maps.

Landslide hazard zone	Number of landslide falling within hazard zone		Percent of landslide falling within hazard zone			
	Grid overlay method	GIS modeling approach	Grid overlay method (%)		GIS modeling approach (%)	
Very high hazard (VHH)	14	15	61	82.73	65.2	95.6
High hazard (HH)	5	7	21.73		30.4	
Medium hazard (MH)	4	1	17.39		4.3	
Low hazard (LOH)	0	0	0.00		0.00	
Very low hazard (VLH)	0	0	0.00		0.00	
Total past landslides	23	23	100		100	

In the case of LHZ map prepared by the 'Grid overlay' method about 82.73% (19 landslides) of past landslides fall within VHH or HH zones whereas in the case of 'GIS modeling' approach about 95.6% (22 landslides) of past landslides fall within VHH or HH zones. Thus, the two methods almost produced the results, which validate with past landslide data, though GIS modeling produced better results. However, in the case of application the 'Grid overlay' method is tedious because of limitations on software and hardware application and is more time consuming whereas, 'GIS modeling' is relatively simple in its application and less time consuming. Thus, the two methods are equally good as far as the result outcome is concerned, though in the present case GIS modeling has given better validation with past landslide activities. However, choice for the two methods can be made based on the area and scale in which the study has to be carried out, as for a large study area at medium scale 'Grid overlay' method may not be appropriate owing to limitations on software and hardware capacity to handle a large number of grid cells. Though, the size of the grid cell will also be a factor to be considered.

7. Conclusion

The main objective of the present study was to evaluate landslide hazard zonation (LHZ) in Meta Robi District in the West Showa Zone in Oromiya Regional State in Ethiopia, which is about 96 km from Addis Ababa. The area is being affected by repeated landslide problems for the past several years therefore seeing the severity of landslide related problems in the area the present research study was conducted. Further, it was also intended to evaluate LHZ by following the 'Grid overlay' method and the 'GIS modeling' approach and to evaluate the relative effectiveness of the two methods.

The general methodology followed in the present study was based on thorough literature review, field investigations, data collection, analysis and evaluation of various causative factors in inducing instability to slopes in the present study area. Finally, preparing LHZ map by using integrated field based GIS 'Grid overlay' method and the 'GIS modeling' approach.

During the field investigation a thorough inventory was made for the past landslide activities to record the locations, dimension, type of failure and material involved in the landslides. The landslide inventory data in general revealed that 23 landslides have occurred in the past in the study area by following four types of prominent failure modes; fall, translational and rotational slides, and complex type of failure modes. Out of total, 83.3% of past landslides have occurred in colluvial soil slopes whereas about 15.2% landslides were observed in alluvial soils. Not many landslides were recorded from slopes formed by rocks. Most of the landslides (52%) occurred in the elevation class of 2132–2382 m whereas, 35% of the landslides occurred in the elevation class of 1632–1882 m. The colluvial and alluvial soils form moderate slopes and much of the landslides (96%) occurred within moderate slope classes. About 70% of past landslides occurred in the hydro-geological homogeneous zone of 1382–1990 m.

In the present study six causative factors namely; slope material, slope, aspect, elevation, land use/land cover and groundwater surface traces were considered. In the present study Landslide Susceptibility Index (LSI) was computed by considering landslide percentage which represents the ratio between ''total pixel counts of a sub-class within a Landslide" to the ''total pixel count of that sub-class in the area of study". The LSI values were calculated for each sub-class of all six causative factors. Later, these LSI values for various causative factors sub-classes were utilized for LHZ evaluation.

For Grid overlay analysis the entire study area was overlaid by a total 7666 polygon grid cells (10×10 m). Later, geoprocessing was done to know the presence of six causative factors within each grid cell. Further, within each grid cell 'Total Landslide susceptibility Index' (TLSI) was computed which was later utilized for Landslide hazard zonation evaluation. The LHZ map thus prepared shows that 19.44% of the study area has a 'very high hazard' (VHH) potential and 30.78% area has 'high hazard' (HH) potential. Whereas, the areas that account for 'medium hazard' (MH), 'low hazard' (LOH) and 'very low hazard' (VLH) are 41.08%, 6.48% and 2.23%, respectively. The validation of LHZ map prepared by the 'Grid overlay' method with past landslides showed 82.73% of the total past landslide activities either falls within VHH or HH zones of the prepared LHZ map. This shows a good validation of the LHZ map with past landslide activities.

The LHZ map prepared by 'GIS modeling' shows that 21.4% of the area falls in VHH zone, 33.2% in HH zone and 34.4% in MH zone. The validation of LHZ map prepared by 'GIS modeling' with past landslides show 95.6% of the total past landslide activities either falls within VHH or HH zones of the prepared LHZ map. This is in close agreement to the past landslides in the area.

On comparison 'Grid overlay' method with 'GIS modeling' for the effectiveness in LHZ evaluation it was realized that 'GIS modeling' has given a better validation with past landslide activities. However, it is concluded that the choice for the selection of the two methods can be made based on area and scale at which the study has to be carried out, as for large study area at medium scale The 'Grid overlay' method may not be appropriate due to the limitations on software and hardware capacity to handle large volumes of data for analysis. Also, the size of the grid cell will also be a factor to be considered while applying grid overlay method for LHZ evaluation.

Acknowledgments

The authors are grateful to the School of Earth Sciences, Addis Ababa University for the support. The authors are grateful to the local respondents and the community residing in the area for providing, important information and the support in the field data collection process.
Further, we are also thankful to the two anonymous esteemed reviewers whose meticulous review work has helped in improving the overall quality of the present research work.

References

Ahmed, S., 2009. Slope Stability Analysis Using GIS and Numerical Modeling Techniques (Unpublished MSc thesis), Vrije Universiteit, Brussel.

Anbalagan, R., 1992. Landslide hazard evaluation and zonation mapping in mountainous terrain. Eng. Geol. 32, 269–277.

Arora, K.R., 1997. Soil Mechanics and Foundation Engineering. Standard Publishers Distributers, Delhi, India.

Assefa, G., 1991. Lithostratigraphy and environment of deposition of the late Jurassic – early cretaceous sequences of the central part of the Northwestern Plateau, Ethiopia. N. Jb. Geol. Palaont. Abh. 182 (3), 255–284.

Ayalew, L., Yamagishi, H., Ugawa, N., 2004. Landslide susceptibility mapping using GIS-based weighted linear combination, the case in Tsugawa area of Agano River, Niigata Prefecture, Japan. Landslides 1, 73–81.

Ayalew, L., Yamagishi, H., 2004. Slope failures in the Blue Nile basin, as seen from landscape evolution perspective. Geomorphology 61, 1–22.

Ayalew, L., Yamagishi, H., 2002. Landslides in the Kakuda-Yahiko Mountains of Niigata, Their Analyses and Description Using GIS. National Congress of Engineering Geological Society of Japan, Takamatsu, Japan, pp. 131–134.

Ayalew, L., 1999. The effect of seasonal rainfall on landslides in the highlands of Ethiopia. Bull. Eng. Geol. Environ. 58, 9–19.

Ayele, S., Raghuvanshi, T.K., Kala, P.M., 2014. Application of Remote Sensing and GIS for Landslide Disaster Management – A case from Abay Gorge, Gohatsion – Dejen Section, Ethiopia. Landscape Ecology and Water Management. In: Proceedings of International Geographical Union (IGU) Rohtak Conference, Advances in Geographical and Environmental Sciences. In: Singh, M., Singh, R.B., Hassan, M.I. (Eds.), Vol 2. Springer, Japan, pp. 15–32.

Ayenew, T., Barbieri, G., 2005. Inventory of landslides and susceptibility mapping in the Dessie area, Northern Ethiopia. Eng. Geol. 77, 1–15.

Bommer, J.J., Rodríguez, C.E., 2002. Earthquake-induced landslides in Central America. Eng. Geol. 63, 189–220.

Carrara, A., Cardinali, M., Guzzetti, F., Reichenbach, P., 1995. GIS Technology in Mapping Landslide Hazard. In: Carrara, A., Guzzetti, F. (Eds.), . In: Geographical Information System in Assessing Natural Hazard. Kluwer Academic Publisher, Netherlands, pp. 135–175.

Carrara, A., Cardinali, M., Guzzetti, F., 1992. Uncertainty in assessing landslide hazard and risk. ITC J. 2, 172–183.

Casagli, N., Catani, F., Puglisi, C., Delmonaco, G., Ermini, L., Margottini, C., 2004. An inventory-based approach to landslide susceptibility assessment and its application to the Virginio River Basin, Italy. Environ. Eng. Geosci. 10 (3), 203–216.

Collison, A., Wade, S., Griffiths, J., Dehn, M., 2000. Modelling the impact of predicted climate change on landslide frequency and magnitude in SE England. Eng. Geol. 55, 205–218.

Crozier, M.J., Glade, T., 2005. Landslide Hazard and Risk: Issues, Concepts, and Approach. In: Glade, T., Anderson, M., Crozier, M. (Eds.), Landslide Hazard and risk. Wiley, Chichester, pp. 1–40.

Dahal, R.K., Hasegawa, S., Masuda, T. Yamanaka, M., 2006. Roadside Slope Failures in Nepal during Torrential Rainfall and their Mitigation. Disaster Mitigation of Debris Flows, Slope Failures and Landslides. pp. 503–514.

Dai, F.C., Lee, C.F., 2002. Landslide characteristics and slope instability modeling using GIS, Lantau Island, Hong Kong. Geomorphology 42, 213–228.

Dai, F.C., Lee, C.F., Ngai, Y.Y., 2002. Landslide risk assessment and management: an overview. Eng. Geol. 64, 65–87.

Dai, F.C., Lee, C.F., 2001. Terrain-based mapping of landslide susceptibility using a geographical information system: a case study. Can. Geotech. J. 38, 911–923.

Dow, D.B., Beyth, M., Hailu, T., 1971. Paleozoic glacial rocks recently discovered in Northern Ethiopia. Geolog. Mag. 108 (l), 53–60.

Fall, M., Azzam, R., Noubactep, C., 2006. A multi-method approach to study the stability of natural slopes and landslide susceptibility mapping. Eng. Geol. 82, 241–263.

Garland, C.R., 1980. Geology of Adigrat area: Ministry of Mines Energy and Water Resources. Memoir l, 51.

Guzzetti, F., Carrara, A., Cardinali, M., Reichenbach, P., 1999. Landslide hazard evaluation: a review of current techniques and their application in a multi-scale study, central Italy. Geomorphology 31 (1–4), 181–216.

Hoek, E., Bray, J.W., 1981. Rock Slope Engineering (Revised Third Edition). Institute of Mining and Metallurgy, London, pp. 358.

Kanungo, D.P., Arora, M.K., Sarkar, S., Gupta, R.P., 2006. A comparative study of conventional, ANN black box, fuzzy and combined neural and fuzzy weighting procedures for landslide susceptibility zonation in Darjeeling Himalayas. Eng. Geol. 85, 347–366.

Keefer, D.V., 2000. Statistical analysis of an earthquake-induced landslide distribution – the 1989 Loma Prieta, California event. Eng. Geol. 58, 231–249.

Lan, X.V., Zhou, C.H., Wang, L.J., Zhang, H.Y., Li, R.H., 2004. Landslide hazard spatial analyst and prediction using GIS in the xiaojiang watershed, Yunnan, China. Eng. Geol. 76, 109–128.

Lee, S., Min, K., 2001. Statistical analysis of landslide susceptibility at Yongin, Korea. Environ. Geol. 40, 1095–1113. http://dx.doi.org/10.1007/s002540100310.

Leroi, E., 1997. Landslide risk mapping: problems, limitation and developments. In: Cruden, Fell. (Ed.), Landslide Risk Assessment. Balkema, Rotterdam, pp. 239–250.

Lineback, G.M., Marcus, W.A, Aspinall, R., Custer, S.G., 2001. Assessing landslide potential using GIS, soil wetness modeling and topographic attributes, Payette River, Idaho. Geomorphology 37, 149–165.

Pachauri, A.K., Pant, M., 1992. Landslide hazard mapping based on geological attributes. Eng. Geol. 32, 81–100.

Pan, X., Nakamura, H., Nozaki, T., Huang, X., 2008. A GIS-based landslide hazard assessment by multivariate analysis. J. Japan Landslide Society 45 (3), 187–195.

Parise, M., Jibson, R.W., 2000. A seismic landslide susceptibility rating of geologic units based on analysis of characteristics of landslides triggered by the 17 January, 1994 Northridge, California earthquake. Eng. Geol. 58, 251–270.

Peng, S.H., Shieh, M., Fan, S.Y., 2012. Potential hazard map for disaster prevention using GIS-based linear combination approach and analytic hierarchy method. J. Geogr. Info. Sys. 4, 403–411.

Raghuvanshi, T.K., Ibrahim, J., Ayalew, D., 2014. Slope stability susceptibility evaluation parameter (SSEP) rating scheme – an approach for landslide hazard zonation. J. Afr. Earth Sci. 99, 595–612.

Sarkar, S., Kanungo, D.P., 2004. An integrated approach for landslide susceptibility mapping using remote sensing and GIS photogram. Eng. Remote Sens. 70 (5), 617–625.

Sarkar, S., Kanungo, D.P., Mehrotra, G.S., 1995. Landslide hazard zonation: a case study in Garhwal Himalaya, India. Mount. Res. Dev. 15 (4), 301–309.

Sidle, R.C., Ochiai, H., 2006. Landslides: Processes, Prediction, and Landuse, 18. American Geophysical Union, Water Resources Monograph, Washington, D.C, pp. 312.

Turrini, C.T., Visintainer, P., 1998. Proposal of a method to define areas of landslide hazard and application to an area of the Dolomites, Italy. Eng. Geol. 50, 255–265.

Varnes, D.J., 1996. Landslide Types and Processes. In: Turner, A.K., Schuster, R.L. (Eds.), Landslides: Investigation and Mitigation, Transportation Research Board Special Report 247. National Academy Press, National Research Council, Washington, D.C.

Wang, X., Niu, R., 2009. Spatial forecast of landslides in three gorges based on spatial data mining. Sensors 9, 2035–2061.

Van Westen, C.J., 1994. GIS in Landslide Hazard Zonation: A Review, with Examples from the Andes of Colombia. In: Price, M. F., Heywood, D.I. (Eds.), . In: Mountain Environments and Geographic Information Systems. Taylor and Francis Publishers, pp. 135–165.

Wieczorek, G.F., Mandrone, G., DeColla, L., 1997. The Influence of Hill-Slope Shape on Debris-Flow Initiation. In: Chen, C.L. (Ed.), Debris-Flow Hazards Mitigation: Mechanics, Prediction, and Assessment. Ame Society of Civil Engg, New York, pp. 21–31.